Journal of
Marine Science and Engineering

MDPI

Article

Experimental Study on the Spring-like Effect on the Hydrodynamic Performance of an Oscillating Water Column Wave Energy Converter

Ning Yuan [1], Chuanli Xu [1] and Zhen Liu [1,2,3,4,*]

[1] Shandong Provincial Key Laboratory of Ocean Engineering, Ocean University of China, Qingdao 266100, China; yuanning@ouc.edu.cn (N.Y.); xuchuanli@stu.ouc.edu.cn (C.X.)
[2] Qingdao Municipal Key Laboratory of Ocean Renewable Energy, Ocean University of China, Qingdao 266100, China
[3] Rizhao Port Group, Rizhao 276826, China
[4] Center for Ocean Carbon Neutrality, Ocean University of China, Qingdao 266100, China
* Correspondence: liuzhen@ouc.edu.cn; Tel.: +86-532-6089-5309

Abstract: The oscillating water column (OWC) wave energy converter has demonstrated significant potential for converting ocean wave energy. The spring-like effect of air compressibility can significantly affect the hydrodynamic behavior of the device, but it has rarely been investigated through experimental studies. In this study, an experimental test on a model-scaled OWC device was carried out in a wave flume using a series of regular and irregular waves. The spring-like effect was taken into account by the combination of the air chamber with an additional air reservoir of appropriate volume, where the total volume was scaled according to the square of the Froude scale. The hydrodynamic performance was compared with the results obtained without considering the spring-like effect. A phase difference between the air pressure and airflow rate was observed when employing the additional air reservoir. The amplitudes of free surface elevation and airflow rate increased, while the air pressure was reduced when the spring-like effect was considered. The results demonstrate that failure to consider the spring-like effect can lead to overestimation of the hydrodynamic efficiencies, and the errors were mainly affected by the incident wave frequency.

Keywords: wave energy; oscillating water column; spring-like effect; air compressibility; hydrodynamic performance

Citation: Yuan, N.; Xu, C.; Liu, Z. Experimental Study on the Spring-like Effect on the Hydrodynamic Performance of an Oscillating Water Column Wave Energy Converter. *J. Mar. Sci. Eng.* **2024**, *12*, 1327. https://doi.org/10.3390/jmse12081327

Academic Editors: Elizaldo Domingues Dos Santos and Liércio André Isoldi

Received: 14 July 2024
Revised: 29 July 2024
Accepted: 4 August 2024
Published: 6 August 2024

1. Introduction

In recent years, ocean wave energy has become a promising form of marine renewable energy for its broad availability, high energy density, and excellent quality [1,2]. Among the various wave energy technologies, the oscillating water column (OWC) wave energy converter has been the most successful due to its simple and reliable device structure [3]. The OWC device converts wave energy via a hollow air chamber partially submerged in water. The water column inside the chamber oscillates vertically through the propagation of incident waves, and then reciprocating airflows are generated. The airflow can drive the air turbine and an electrical generator that ultimately produce electricity [4]. The main advantage of OWC compared to other wave energy devices is that there are no moving parts underwater.

The concept of OWC was first introduced in the 1940s, and since then, a large number of devices have been extensively researched and developed around the world [5]. The first application of OWC technology was to power navigation buoys invented by Yoshio Masuda, which was undoubtedly successful as it achieved commercial application in Japan and other countries [6]. This was followed by the invention of a large floating OWC called Kaimei. It was then deployed off the west coast of Japan [7]. In Europe, a small shoreline

OWC plant equipped with a 75 kW Wells turbine was built on the coast of Islay Island in Scotland in the 1990s. After that, the LIMPET OWC, with a rated power of 500 kW, was commercially installed on the shoreline of Islay [8]. Another prototype, the OWC, named the Pico OWC plant, was constructed on the island of Pico in Portugal. The plant started operating in 1999 and was destroyed by a sea storm in 2018 [9]. At present, some prototype OWC plants, such as the Mutriku wave power plant and the YongSoo OWC plant, have been constructed, are still in operation, and have achieved good commercial demonstration [10,11].

The studies on the design of the OWC chamber were conducive to improving the energy capture efficiency. Simonetti and Cappietti [12] assessed the effectiveness of the OWC chamber by considering the effect of design parameters. The results show that the converting performance was primarily influenced by the chamber length and the incident wavelength. It was found that the floating OWC was able to convert more wave energy in the deep sea [13,14]. Giorgi et al. [15] investigated the hydrodynamic performance of a floating spar-buoy OWC and found that the parametric resonance could lead to a significant reduction in conversion efficiency. The multiple OWC chambers have also been employed to improve the hydrodynamic performance. Kim et al. [16] conducted an experimental study on multiple chambers and found that triple chambers contributed to better performance due to reducing the sloshing motion of the water column. Recently, wave-wo-wire models have been proposed to better design the entire OWC system. Liu et al. [17] established an integrated numerical model that linked the turbine and air chamber in a transient model. Ciappi et al. [18] applied a comprehensive wave-to-wire model to evaluate the energy output of an OWC plant, and the effect of Wells turbines and impulse turbines on overall performance was compared. A non-linear time-domain wave-to-wire model was developed, and the control strategies of the air turbine and electrical generator were performed [19].

It is noteworthy that most previous investigations of OWC have been focused on small-scale models, and very few tests were conducted on large-scale or full-sized prototypes. However, the air is difficult to compress in the small OWC model because of volume limitations. In the prototype OWC, the air inside the chamber is often compressible, and the density changes during the exhalation and inhalation processes, which is called the spring-like effect of air compressibility [20]. It has been shown that ignoring air compressibility tends to introduce considerable error in predicting the performance of the OWC [21,22]. Sheng et al. developed analytical formulations of the thermodynamics of air inside the OWC chamber and reported the power loss due to the spring-like effect when airflow reaches the power take-off (PTO) [23]. Şentürk and Özdamar studied the effects of air compressibility numerically and found that the incompressible model results in a 30% error in airflow velocity [24]. Thakker et al. investigated the compressibility effects inside the OWC device, and the results show that the mean conversion efficiency was reduced by 5% when the air was compressible [25]. Gonçalves et al. compared the spring-like effect on the OWC efficiency in relation to incident wave period and turbine damping by numerical study and found an overestimation of 20% in converting efficiency if the spring-like effect is ignored [26]. Elhanafi et al. studied the scaling and air compressibility effects on an offshore OWC by employing five different model scales and reported that the air compressibility can be ignored when the scale is less than 1:10. In addition, ignoring the air compressibility effects leads to a 12% overestimation in converting efficiency and changes the optimum PTO damping [27].

Evaluating the spring-like air compressibility effect and thus correcting the hydrodynamic errors in the small-scale model is very important for accurately predicting OWC performance. Sarmento and Falcão analyzed the air compressibility effect based on linear surface-wave theory and proposed that air compressibility can be reproduced if the height of the air chamber is increased appropriately [28]. Later, Weber carried out physical tests and reported that the height of the air chamber was a key factor affecting air compressibility. An alternative method of reproducing the air compressibility is to add an additional volume

to the air chamber [29]. Therefore, the conventional Froude similarity law is no longer applicable when the air compressibility effect is considered in a scale model [30]. Dimensional analysis indicated that to accurately model air compressibility, the volume of the air chamber should be scaled by the square of the scale ratio instead of the cube [30,31]. This means that a larger volume of air chamber is required to maintain air pressure similarity in a small-scale model. A typical method to accomplish this is by linking the air chamber to a rigid air reservoir of suitable volume [31,32].

Fairhurst et al. added an auxiliary volume to the air chamber to introduce the effect of air compressibility in experimental tests and optimized the performance of a submerged OWC device [33]. Perez-Collazo et al. conducted 1:50 scale model tests of a hybrid wind-wave energy converter. An air reservoir was attached to the OWC chamber to account for air compressibility [34]. Howe et al. investigated the spring-like effect of a 1:20 bent duct-type OWC device and studied the effects of added chamber volumes experimentally [35]. Benreguig and Murphy predicted the performance of the Tupperwave OWC, and the external reservoir, scaled by the square of the scale ratio, was used to reproduce air compressibility [36]. Rosa-Santos et al. integrated the OWC into the harbor breakwater and evaluated the hydrodynamic performance of this hybrid device. An air reservoir was utilized in the tests to accurately account for air compressibility [37]. López et al. studied the air compressibility effects by scaling the chamber using both the cube and the square of the scale. The results showed that neglecting air compressibility could result in either an underestimation or an overestimation of the performance [38]. Portillo et al. carried out experimental tests of a floating coaxial-duct OWC and found that the contributions of air compressibility to the absorption performance were dependent on the wave frequency [39,40].

With the rapid development of wave energy technology, it is particularly important to accurately predict the energy conversion performance of devices. However, from the literature review, it can be concluded that most research on OWC has not considered the effects of air compressibility, which can lead to errors in predicting the performance of the device and fail to guide precise design. In this study, a rectangular OWC device, which takes into account the spring-like effect of air compressibility by scaling the air chamber with the square of the scale ratio, was experimentally tested in a wave flume. The spring-like effects on the free surface elevation, airflow rate, air pressure, and hydrodynamic efficiency were investigated and compared. The main motivation of this work is to evaluate the spring-like effect of air compressibility and quantify its impact on the converting performance of the OWC device, which can help to more accurately predict the energy output of the device and assess its economics when designing the prototype plant.

2. Model Design and Experimental Setup

2.1. Similarity Criterion of the Air Chamber Volume

For an OWC system, the air mass m inside the air chamber is considered as:

$$m = \rho_{ch} V \tag{1}$$

where ρ_{ch} is the air density in the chamber, and V is the air volume of the chamber. The mass flow rate passing over the PTO device can be written as:

$$w = \frac{dm}{dt} = V \cdot \frac{d\rho_{ch}}{dt} + \rho_{ch} \cdot q \tag{2}$$

where q is the volume flow rate and is defined as $q = dV/dt$. The positive and negative values of q represent the flow rate during the inhalations and exhalations, respectively. Typically, higher values of the performance parameters are achieved during the outflow phase than the inflow phase due to the higher air density. The first item of Equation (2) on the right can be employed to represent the effect of air compressibility. To maintain the

dynamic similarity, the ratio of two items on the right τ should be the same in both the model and prototype scales [31], where τ is written as:

$$\tau = \frac{V}{\rho_{ch} \cdot q} \cdot \frac{d\rho_{ch}}{dt} \tag{3}$$

In an open system, air density is supposed to be a function of pressure. The assumption is that the airflow is isentropic in the chamber [28] and can be written as:

$$\frac{p_{ch}}{\rho_{ch}^{\gamma}} = \text{constant} \tag{4}$$

where p_{ch} is the air pressure in the chamber and γ is the air-specific heat ratio, commonly γ = 1.4. From Equation (4), at any moment during the inhalation or exhalation,

$$\frac{p_{\text{at}} + p}{\rho_{ch}^{\gamma}} = \frac{p_{\text{at}}}{\rho_{at}^{\gamma}} \tag{5}$$

where p is the pressure oscillation in the chamber, and $p_{ch} = p_{at} + p$. p_{at} and ρ_{at} are the atmospheric pressure and air density of the environmental atmosphere, respectively. From Equation (5), it is derived that:

$$\rho_{ch} = \rho_{\text{at}} \left(1 + \frac{p}{p_{at}}\right)^{\frac{1}{\gamma}} \tag{6}$$

In a small-scale OWC model, the oscillation of air pressure p in the chamber is assumed to be much less than p_{at}. Then, the linearized form of Equation (6) by means of the Taylor expansion can be derived as:

$$\rho_{ch} = \rho_{\text{at}} \left(1 + \frac{p}{\gamma \cdot p_{at}}\right) \tag{7}$$

The time derivative of Equation (7) is written as:

$$\frac{d\rho_{ch}}{dt} = \frac{\rho_{at}}{\gamma \cdot p_{at}} \cdot \frac{dp}{dt} \tag{8}$$

Bringing Equation (8) into Equation (3), it can be derived as:

$$\tau = \frac{V}{\gamma \cdot q(p + p_{at})} \cdot \frac{dp}{dt} \tag{9}$$

Since τ should be equal in the prototype and model scales, it can be derived as:

$$\frac{V_m}{V_p} = \frac{q_m}{q_p} \cdot \frac{p_m + p_{at,m}}{p_p + p_{at,p}} \cdot \frac{(dp/dt)_p}{(dp/dt)_m} \tag{10}$$

and the subscripts m and p represent the model and prototype. According to the similarity theory:

$$\frac{q_m}{q_p} = \lambda_L^{2.5}, \ \frac{p_m}{p_p} = \lambda_L^{2.5} \cdot \lambda_{\rho w}, \ \frac{(dp/dt)_m}{(dp/dt)_p} = \lambda_L^{0.5} \cdot \lambda_{\rho w} \tag{11}$$

where λ_L and $\lambda_{\rho w}$ are the length scale and the scale of water density, respectively.

If Equation (10) conforms to the Froude similarity criterion, bringing Equation (11) into Equation (10), it should be satisfied with $V_m/V_p = {\lambda_L}^3$ as $p_{at,\,m}/p_{at,\,p} = \lambda_L \cdot \lambda_{\rho w}$, where $\lambda_{\rho w}$ = 1. This means that the ratio of the atmosphere pressure between the model and prototype scales should equal the length scale, which is evidently improper. A reasonable

assumption is that $p_{at,\,m} = p_{at,\,p}$, and the pressure oscillation p is negligible compared to p_{at}. Subsequently, it can be derived as:

$$\frac{V_m}{V_p} = \lambda_L^2 \cdot \lambda_\rho^{-1} = \lambda_L^2 \tag{12}$$

If the pressure oscillation p is large and not negligible compared to p_{at}, this means that the scale is large enough and the airflow in the air chamber is compressible, and then the scale effect can be ignored. This indicates that the ratio of chamber volume between the model and prototype scales should be the square of the length ratio.

2.2. Model Design of the Air Chamber

As gravity plays a dominant and crucial role in the physical tests of the OWC device, the Froude similarity criterion is recommended as the primary similarity law [31]. A scale ratio of λ_L = 1:10 was chosen in this experimental model. A classic rectangular OWC air chamber was used in this study to make the results more representative, as shown in Figure 1a, and the length, width, and height of the chamber were 0.4 m, 0.8 m, and 1.0 m, respectively. A hole with a circular shape and a diameter measuring 0.1 m was punctured in the center of the top wall, and an air duct with a length of 0.3 m was connected to the hole. In addition to the wave excitation force, the OWC device is also subjected to PTO damping force and added mass force. The damping force exerted by the PTO is determined by the air pressure oscillation in the chamber and the cross-sectional area of the air chamber, and the added mass force is generated by the oscillation of the water column [41]. In the case of small-scale OWC devices, the impulse turbine is generally simulated by an orifice to provide a non-linear damping effect [31]. It should be noted that the size of the orifice and the resulting pneumatic damping will have an effect on the air pressure and the free surface elevation inside the chamber, thus determining the energy capture of the OWC device. In this model, the orifice area was taken as 1% of the water column area inside the air chamber, and research has shown that the device could achieve high energy conversion performance around this orifice size [42].

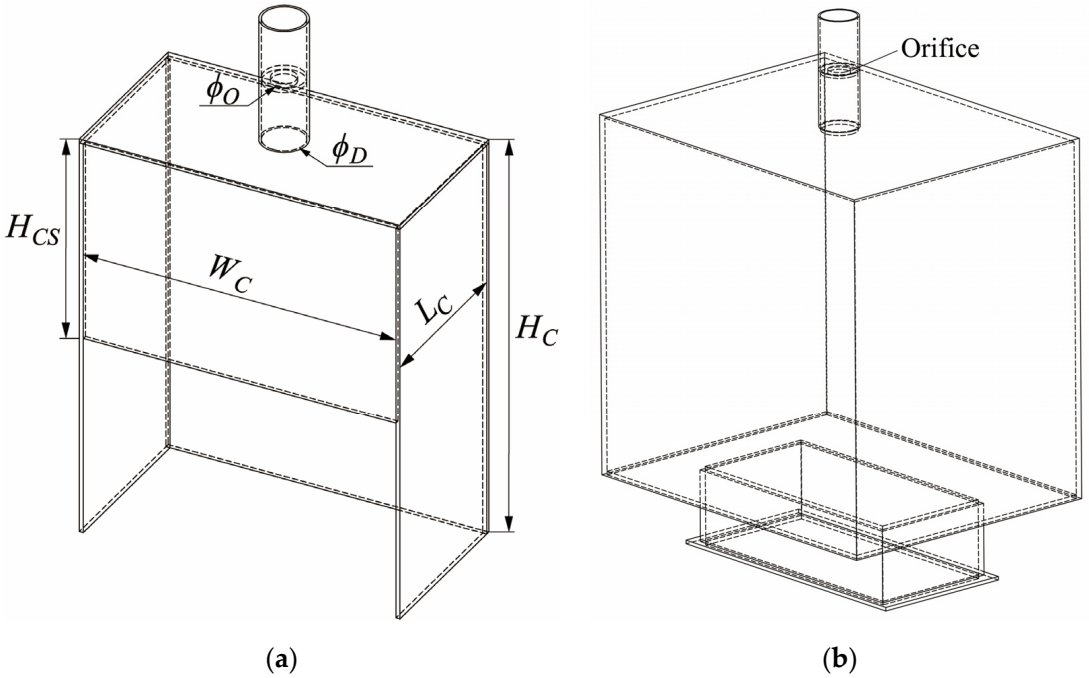

Figure 1. Sketch of the OWC model. (**a**) Air chamber; (**b**) air reservoir with additional volume.

Two different setups of the air chamber were conducted in this test. In the first case, the volume of the air chamber was scaled by the cube of the scale ratio when the spring-like effect was ignored, and the chamber volume was 0.096 m^3. According to the results of Section 2.1, the air volume should be scaled by the square of the scale ratio when the air compressibility effect is considered. In the second case, the total volume of air was 0.96 m^3. In order to directly compare the effect of air compressibility, instead of reshaping the air chamber, the top wall was removed and connected to an appropriately sized air reservoir. Deducting the original air chamber, the additional air chamber volume containing the air reservoir and connecting part was equal to 0.864 m^3. The air reservoir was made of 15 mm thick acrylic plates, which can ensure that the volume remains unchanged as the internal pressure oscillates. In the compressible cases, the air duct containing the orifice was mounted on the top of the reservoir, as shown in Figure 1b. The detailed geometrical parameters of the model are listed in Table 1.

Table 1. Parameters of the OWC device.

Definition	Symbol	Value	Definition	Symbol	Value
Chamber height	H_C	1.0 m	Skirt height	H_{CS}	0.5 m
Chamber length	L_C	0.4 m	Chamber width	W_C	0.8 m
Diameter of duct	ϕ_D	0.1 m	Diameter of orifice	ϕ_O	0.064 m
Air chamber thickness	T_C	0.01 m	Reservoir thickness	T_R	0.015 m
Air chamber volume	V_C	0.096 m^3	Reservoir volume	V_R	0.0864 m^3

2.3. Experimental Setup

The experimental tests were conducted in a wave flume at the Shandong Provincial Key Laboratory of Ocean Engineering. The flume is 60.0 m in length, 1.5 m in height, and 3.0 m in width. The flume is divided by a glass wall into a 0.8 m wide section and a 2.2 m wide section. The OWC model was placed in the 0.8 m wide section, matching the width of the test section. The experimental setup of the first case, i.e., ignoring the spring-like effect, is illustrated in Figure 2. A piston-type wave maker is installed in the flume to generate desired incident waves, and a wave absorber made of porous media materials is used to dissipate incoming waves. The OWC device was fixed to the bottom of the flume at a distance of 50.0 m from the wave maker. The water depth (h) was maintained at 0.7 m during the tests, with the draft fixed at 0.2 m.

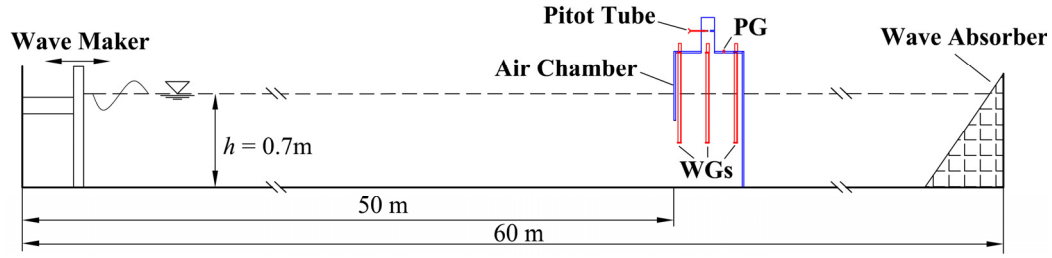

Figure 2. Layout of the experimental setup in the wave flume.

The air chamber was constructed from acrylic plates, and the physical photo of the OWC model can be found in Figure 3. Three capacitance-type wave gauges were positioned at the top of the chamber in the direction of the incident waves to measure the free surface elevation inside the chamber. The distance of the wave gauges from one side wall was 0.2 m, with one gauge placed in the center of the chamber and the other two on either side, 0.15 m from the center. A circular opening on the top wall was used to connect the pressure gauge for measuring the pressure difference. The center of the hole was 0.2 m from the other side wall. All the gauges were linked to a data acquisition system to enable synchronized data acquisition. When conducting tests that take into account the spring-like effect, the air chamber was connected to the additional air reservoir, as shown in Figure 3b.

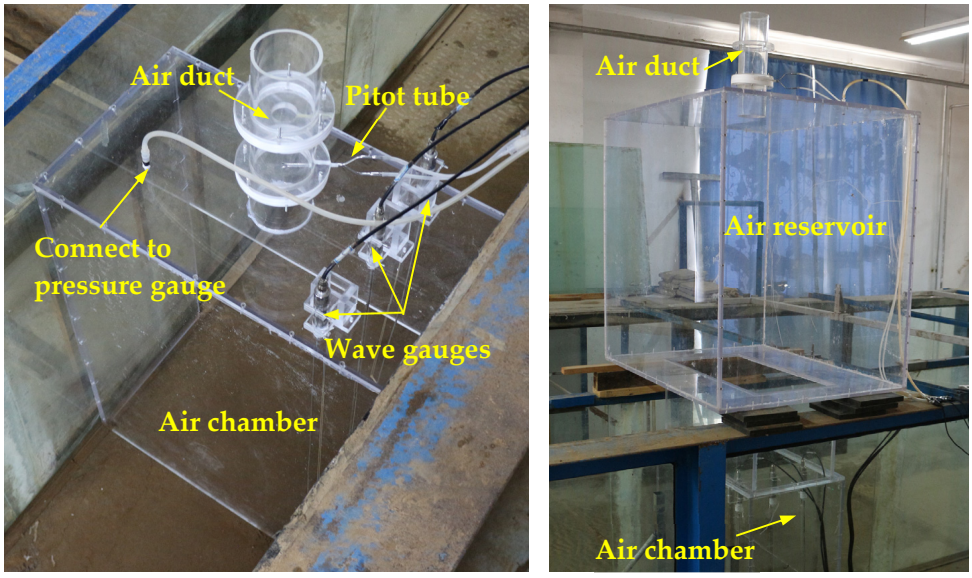

(**a**) (**b**)

Figure 3. Physical photo of the testing device. (**a**) Setup without air reservoir; (**b**) setup with air reservoir.

There are usually two ways of measuring the airflow rate during the opereting process of OWC. The most common is to displace by the motion of the free surface elevation inside the air chamber. However, this method is no longer appropriate when the spring-like effect is considered, as there will be a phase difference between the pressure oscillation and the airflow rate displaced by the free surface elevation, which will result in incorrect power output [21]. Another way to determine the airflow rate is to use Pitot tubes to measure the airflow velocity of a given plane. In this study, a back-to-back Pitot tube was put in the air duct to measure the bidirectional velocity passing the PTO.

The wave conditions tested in this study were designed according to the wave climate of a typical offshore area of North China. Both regular and irregular wave conditions were employed during the tests: fifteen sets of regular waves with three wave heights H = 0.05 m, 0.1 m, and 0.15 m and five wave periods T = 1.25 s to 2.25 s with 0.25 s increments; five sets of irregular waves with a significant wave height H_S = 0.10 m and five significant periods T_S = 1.25 s to 2.25 s with 0.25 s increments. The calculation of the wave power, the pneumatic power, and the energy conversion efficiency can be found in Reference [17]. The cases that disregarded the spring-like effect were tested first, followed by the connection of the air reservoir to the air chamber for testing the compressible cases. Each test case was repeated three times to ensure accuracy and reliability, and the final result was obtained by calculating the average value.

3. Experimental Results and Discussion

3.1. Phase Difference between Airflow Rate and Air Pressure Oscillation

The air compressibility affects the energy conversion performance of the OWC device primarily by affecting both the air pressure and the airflow rate generated by the chamber. In addition, it is important to note that the airflow rate displaced by the oscillation of the free surface elevation exhibits a phase difference with the pressure oscillation when the spring-like effect is considered [31]. In general, a larger phase difference indicates a more pronounced effect of air compressibility. In this section, the phase difference between the air pressure and airflow rate is presented, and the spring-like effect is evaluated.

A typical regular case of H = 0.05 m and T = 1.75 s was chosen to display the time histories of air pressure oscillation and airflow rate displaced by the motion of the free surface elevation, as illustrated in Figure 4. It can be seen that in the incompressible case

without an additional air reservoir, the air pressure oscillation is always in phase with the airflow rate. However, when considering the air compressibility, a significant phase difference is created between them, as shown in Figure 4b. This is due to the fact that when the air is compressible, the airflow generated by the free surface creates a certain delay when it reaches the PTO. According to the calculation equation, pneumatic power is the product of air pressure and flow rate, and the phase difference between them will lead to a negative error value for the power.

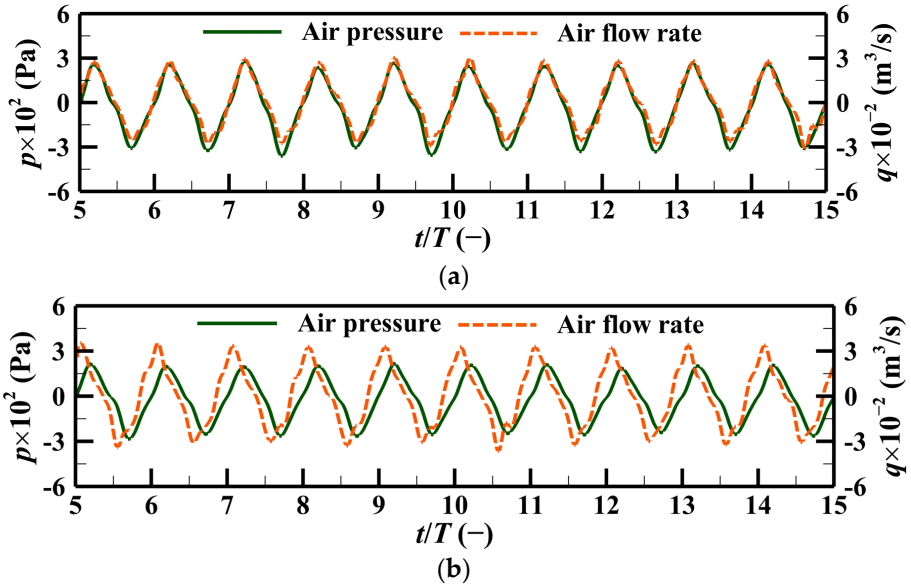

Figure 4. Time histories of the air pressure oscillation and airflow rate (H = 0.05 m and T = 1.75 s). (**a**) Ignoring the spring-like effect; (**b**) considering the spring-like effect.

In this case, when ignoring the spring-like effect, the average values of air pressure and airflow rate amplitude are 320 Pa and 0.032 m^3/s, respectively. In the case of an additional reservoir, the values changed to 281 Pa and 0.035 m^3/s, respectively. The spring-like effect leads to a reduction in the air pressure, an increase in the free surface elevation inside the chamber, and the resulting airflow rate. A similar phenomenon has been reported in theoretical investigations [21].

In cases with additional reservoirs, the phase differences between the air pressure oscillation p and the airflow rate q displaced by the free surface elevation under regular waves are plotted in Figure 5. The non-dimensional parameter $\Delta D/T$ is used to represent the phase difference, where ΔD is the average value of the phase difference between the crests of p and q and the troughs of p and q in ten wave cycles. The wave period is represented by kh, where k is the wave number according to the corresponding period. It can be seen that for any wave height, the phase difference increases as the wave frequency kh increases. In the low-frequency domain, the values of phase difference are about 0.1 times the wave period, while in the high-frequency domain, the phase differences can be up to 0.2 T. The results indicate that wave frequency is a key parameter affecting air compressibility, and the spring-like effect on the performance of the OWC device is more evident at high wave frequencies because of the faster air exchange process. Furthermore, the phase differences tend to be equal for wave heights H = 0.05 m and 0.1 m and become larger for H = 0.15 m. This is because the amplitudes of free surface elevation and air pressure are greater at high wave height, which reinforces the spring-like effect. It should be noted that the phase difference between p and q will result in errors in pneumatic power calculation. This means that in compressible cases, the airflow rate should not be derived from the motion of the free surface but directly from the flow rate through the PTO.

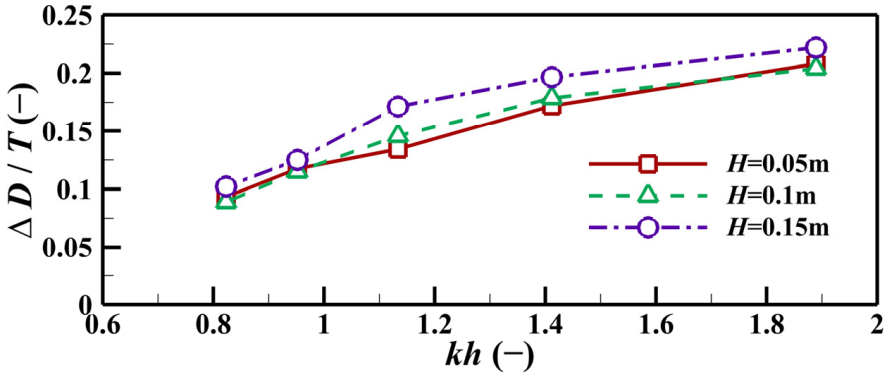

Figure 5. Averaged phase difference between air pressure and airflow rate.

3.2. Spring-like Effect on the Hydrodynamic Performance in Regular Waves

In this section, the spring-like effect on the energy conversion process of the OWC under regular wave conditions is investigated. The free surface elevation inside the chamber is a crucial parameter that reflects the performance, which determines the airflow rate through the PTO and thus affects the aerodynamic energy captured from the waves. The non-dimensional relative free surface elevation amplitudes a/A for various wave conditions under two tests are compared in Figure 6, where a represents the elevation amplitude in the chamber and A is the incident wave amplitude. The percentages in the graph represent the error of the incompressible results (without a reservoir) compared to the results considering a spring-like effect (with an additional reservoir).

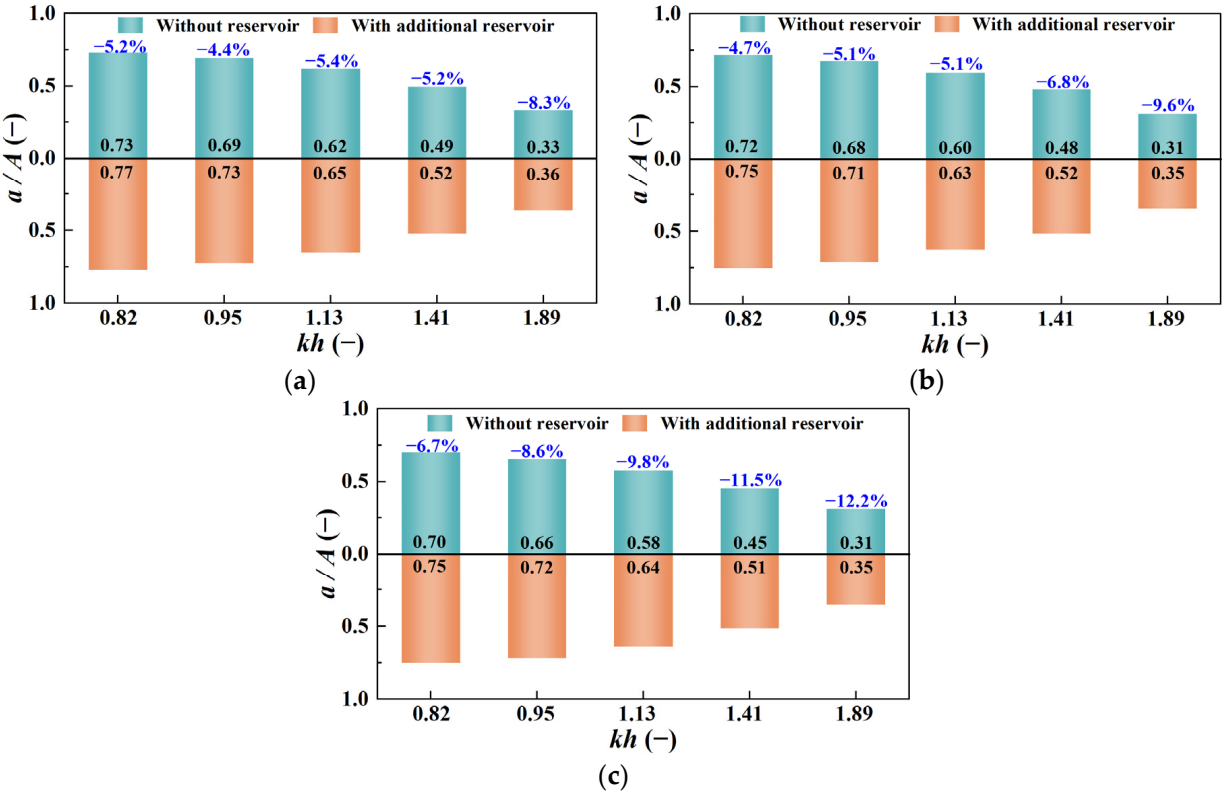

Figure 6. Comparison of relative free surface elevation inside the chamber in regular waves. (**a**) H = 0.05 m; (**b**) H = 0.10 m; (**c**) H = 0.15 m.

Generally, the a/A increases for all wave frequencies when the spring-like effect is taken into account. This is because the damping effect of the air acting on the water column inside the chamber is reduced when the air is compressible, which leads to an increase

in the elevation amplitude. The average reductions in a/A for five wave frequencies in incompressible cases are 5.7%, 6.2%, and 9.8% for wave height H = 0.05 m, 0.1 m, and 0.15 m, respectively. For a given wave height, the spring-like effect is greater in the high wave frequency kh domain. The error of a/A at kh = 1.89 is about twice that of kh = 0.82.

The airflow rate in an OWC device is generated by the oscillation of the free surface. According to the results from Section 3.1, the airflow rate displaced by the motion of the free surface elevation has a phase difference with the air pressure oscillation, which results in incorrectly predicting results. In this test, a Pitot tube was used to directly measure the airflow rate through the PTO, and the results are presented in Figure 7, where Q represents the average amplitude of the airflow rate. The results show that the airflow rate decreases with an increase in wave frequency, and the minimum and maximum values are all obtained at kh = 1.89 and 0.82. In addition, compared to the results with an additional air reservoir, the free surface elevation is reduced in the incompressible cases, which results in a reduction in the airflow rate. The reduction is more obvious at high wave frequencies because the air is more easily compressed during small wave periods. For the three wave heights, the average errors of airflow rate amplitude due to disregarding the spring-like effect are 5.1%, 5.8%, and 9.5%, respectively. This suggests that the spring-like effect increases with increasing wave height, mainly due to the greater interaction of the wave with the OWC device.

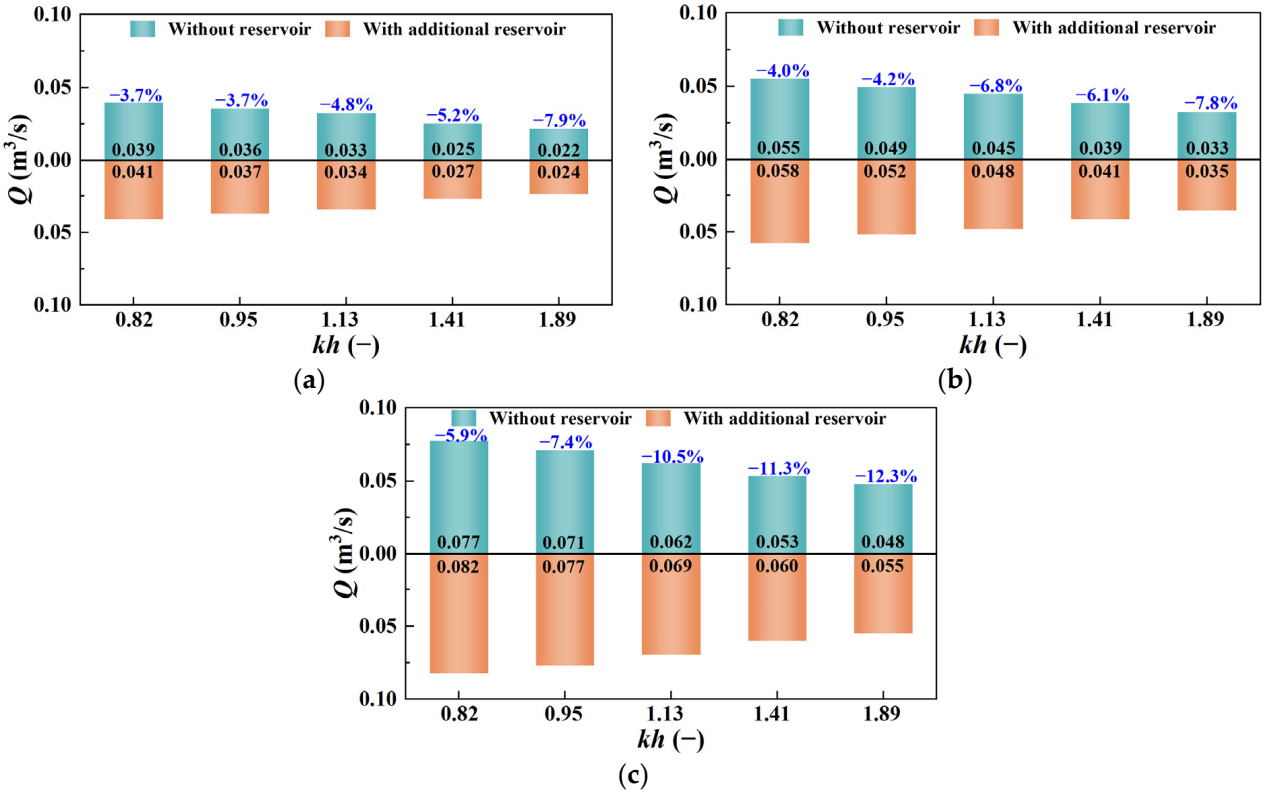

Figure 7. Comparison of airflow rate amplitude in regular waves. (**a**) H = 0.05 m; (**b**) H = 0.10 m; (**c**) H = 0.15 m.

Another crucial parameter influencing energy harvesting is the air pressure in the chamber. The average air pressure amplitude in regular waves is illustrated in Figure 8. The variation pattern is similar to that of the free surface elevation, and the pressure amplitude decreases as the incident wave frequency increases. When the spring-like effect is neglected, the air pressure increases significantly even though the airflow rate is reduced. This is due to the fact that the damping effect is enhanced when the air is incompressible, which consequently induces an increase in the air pressure. When H = 0.05 m, the errors of air pressure due to ignoring the spring-like effect vary from 10.5% to 21.4%, which is much

larger than the errors of free surface elevation and airflow rate. The errors are larger at high wave heights; for H = 0.1 m and 0.15 m, the errors vary from 12.0% to 24.6% and 13.5% to 29.8%, respectively. It can be seen that the influence of the spring-like effect increases as the wave height increases, mainly because the range of variation in air density is greater as the wave height increases. These results indicate that in the small-scale OWC model, ignoring the spring-like effect tends to overestimate the air pressure in the chamber, with the maximum error being close to 30%.

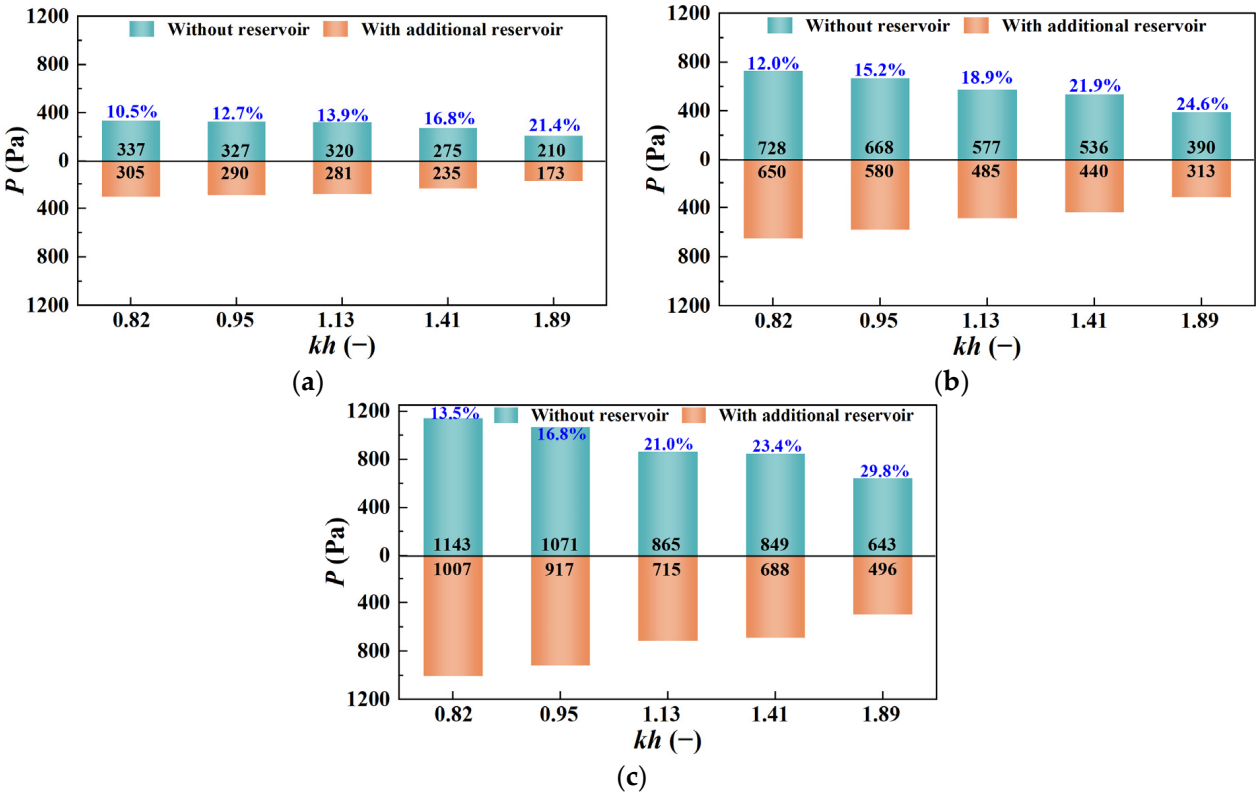

Figure 8. Comparison of air pressure amplitude inside the chamber in regular waves. (**a**) H = 0.05 m; (**b**) H = 0.10 m; (**c**) H = 0.15 m.

The hydrodynamic efficiencies η for various wave conditions considering the spring-like effect are compared in Figure 9. For a given wave height, the efficiency η initially increases and then decreases as the wave frequency kh increases, reaching a peak at kh = 1.41. The results show that the wave frequency is the key parameter affecting the efficiency of the OWC device. The length of the chamber should be specifically designed to resonate with the dominant wave frequency. In addition, ignoring the air compressibility leads to a significant overestimation of η. The spring-like effect is more obvious in the case of large wave heights and high wave frequencies due to more intense interactions between incident waves and the air chamber. For the test wave heights, the average errors η due to ignoring the spring-like effect are 9.2%, 11.4%, and 13.5%, respectively. The maximum error is 18.0%. The results indicate that when predicting the performance of an OWC plant, the results from a small-scale model that ignores the spring-like effect would introduce large errors, and therefore, corresponding corrections are required.

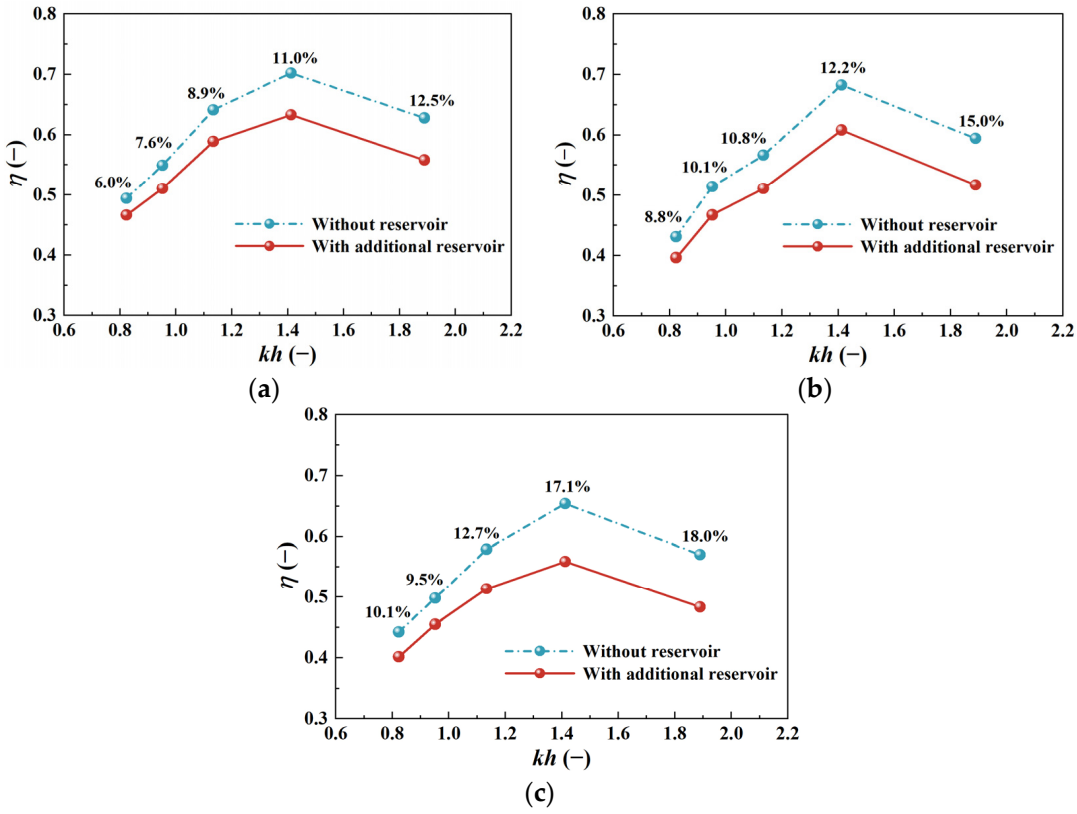

Figure 9. Comparison of hydrodynamic efficiencies in regular waves. (**a**) H = 0.05 m; (**b**) H = 0.10 m; (**c**) H = 0.15 m.

3.3. Spring-like Effect on the Hydrodynamic Performance in Irregular Waves

To offer more valuable insights for performance prediction, the spring-like effect on the OWC performance in irregular waves was also investigated. The free surface amplitudes and airflow rates in irregular waves are shown in Figure 10, where h_S and Q_S represent the significant values of the free surface elevation and significant airflow rate amplitudes, respectively. k_S is the wave number according to the significant wave period. Similar to the results from regular waves, the free surface elevation and airflow decrease as the wave frequency increases. As shown in the figures, the free surface elevation and airflow rate are underestimated when the air compressibility is ignored. In this test, the errors of free surface elevation and airflow rate between the two tests range from 5.9% to 8.7% and 5.1% to 9.1%, respectively.

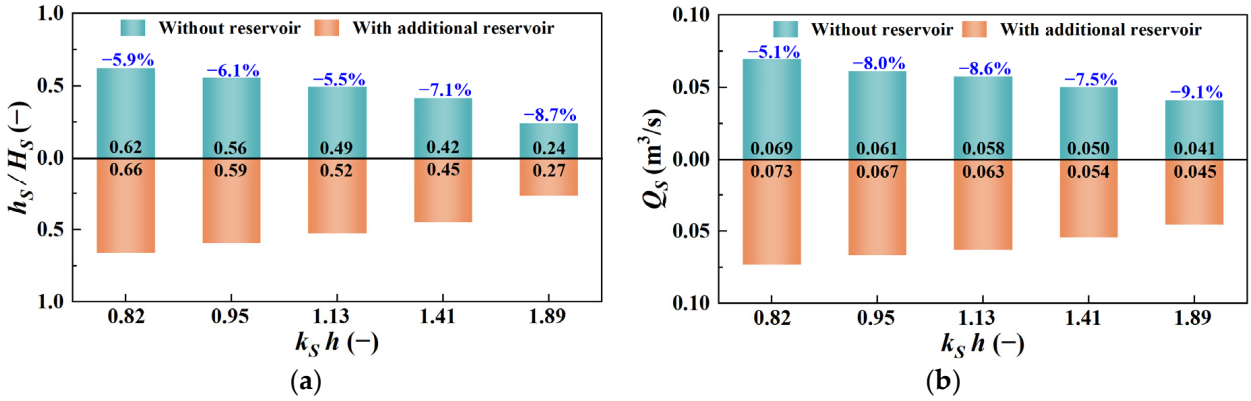

Figure 10. Comparison of hydrodynamic performance in irregular waves (H_S = 0.1 m). (**a**) Relative free surface elevation; (**b**) significant airflow rate.

The significant air pressure amplitude (P_S) is illustrated in Figure 11. The air pressure amplitude also decreases as the wave frequency increases. Additionally, the air pressure amplitude will be overestimated if the spring-like effect is not taken into account. In the low-frequency domain, the error is less than 10%, while in the high-frequency domain, the error of air pressure can be up to 15.9% because of the larger air density variation. Compared to the free surface elevation and airflow rate, the air pressure error caused by ignoring the spring-like effect is larger.

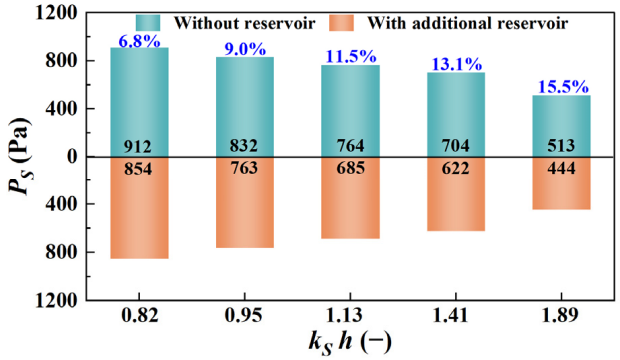

Figure 11. Comparison of significant air pressure amplitude in irregular waves (H_S = 0.1 m).

The spring-like effect on the hydrodynamic efficiencies η in irregular wave conditions is compared in Figure 12. It can be seen that the wave frequency has a significant effect on the η, and the chamber achieves peak efficiency at kh = 1.41 for both the incompressible and compressible cases, which indicates that the spring-like effect will not change the resonance period. The test results show that ignoring the spring-like effect overestimates the energy conversion efficiency of the OWC device, and the effect increases as the wave frequency increases. In the irregular wave test, the error η introduced by ignoring the spring-like effect varies from 4.7% to 10.7%.

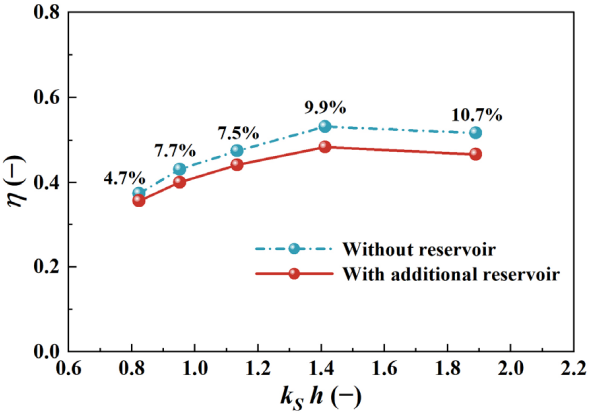

Figure 12. Comparison of hydrodynamic efficiencies in irregular waves (H_S = 0.1 m).

4. Conclusions

In this study, a small-scale OWC model was experimentally tested to investigate the spring-like effect of air compressibility. To take into account the air compressibility, the air chamber volume was scaled by the square of the scale ratio by adding an additional air reservoir. The free surface elevation, airflow rate, air pressure, and hydrodynamic efficiency were illustrated and compared with the results in incompressible cases. The following conclusions can be drawn:

1. The spring-like effect induces a phase difference between the air pressure oscillation and the airflow rate displaced by the motion of the free surface elevation. The

phase difference increases as the wave frequency increases due to the faster air exchange process.
2. When the spring-like effect is not involved, the free surface elevation and the airflow rate are underestimated, and the average errors in regular waves are 7.2% and 6.8%, respectively. On the contrary, the air pressure in the chamber is overestimated by an average of 18.2%.
3. The air compressibility does not change the resonant period of the air chamber, but failure to reproduce it will result in an overestimation in the hydrodynamic efficiency. The average error introduced by the spring-like effect on the efficiency is 11.4% for regular waves and 8.1% for irregular waves.
4. The results suggest that if the conventional Froude similarity law is used when evaluating the OWC device, the pneumatic outputs should be corrected, and a reduction in conversion performance should be considered.

It should be noted that an orifice was used to simulate the damping effect of the air turbine, and the interactions between the turbine and the air chamber were ignored, which may not reflect the real operating condition of the OWC device. In the future, numerical models integrating the real turbine and air chamber can be built to investigate the spring-like effect on the whole process of energy conversion. Furthermore, models at different scales, including large-scale models, shall be considered to investigate the scale effects of the OWC device.

Author Contributions: Conceptualization, N.Y. and Z.L.; methodology, Z.L.; software, N.Y.; validation, C.X.; formal analysis, C.X.; investigation, N.Y.; resources, Z.L.; data curation, N.Y.; writing—original draft preparation, N.Y.; writing—review and editing, C.X. and Z.L.; visualization, C.X.; supervision, Z.L.; project administration, Z.L.; funding acquisition, Z.L. All authors have read and agreed to the published version of the manuscript.

Funding: This research was funded by the Shandong provincial major basic research project of the Natural Science Foundation, grant number ZR2021ZD23; the National Key R&D Program of China, grant number 2023YFB4204104; the National Natural Science Foundation of China, grant number U1906228; the Young top-notch talent project of the National Ten Thousand Talent Program; and the Program of Introducing Talents of Discipline to Universities, grant number B14028.

Institutional Review Board Statement: Not applicable.

Informed Consent Statement: Not applicable.

Data Availability Statement: Data are contained within the article.

Conflicts of Interest: Author Zhen Liu was employed by the company Rizhao Port Group. The remaining authors declare that the research was conducted in the absence of any commercial or financial relationships that could be construed as a potential conflict of interest.

References

1. Khojasteh, D.; Shamsipour, A.; Huang, L.; Tavakoli, S.; Haghani, M.; Flocard, F.; Farzadkhoo, M.; Iglesias, G.; Hemer, M.; Lewis, M.; et al. A Large-Scale Review of Wave and Tidal Energy Research over the Last 20 Years. *Ocean Eng.* **2023**, *282*, 114995. [CrossRef]
2. Zhang, Y.; Zhao, Y.; Sun, W.; Li, J. Ocean Wave Energy Converters: Technical Principle, Device Realization, and Performance Evaluation. *Renew. Sustain. Energy Rev.* **2021**, *141*, 110764. [CrossRef]
3. Rosati, M.; Henriques, J.C.C.; Ringwood, J.V. Oscillating-Water-Column Wave Energy Converters: A Critical Review of Numerical Modelling and Control. *Energy Convers. Manag. X* **2022**, *16*, 100322. [CrossRef]
4. Falcão, A.F.O.; Henriques, J.C.C.; Gato, L.M.C. Self-Rectifying Air Turbines for Wave Energy Conversion: A Comparative Analysis. *Renew. Sustain. Energy Rev.* **2018**, *91*, 1231–1241. [CrossRef]
5. Falcão, A.F.O.; Henriques, J.C.C. Oscillating-Water-Column Wave Energy Converters and Air Turbines: A Review. *Renew. Energy* **2016**, *85*, 1391–1424. [CrossRef]
6. Falcão, A.F.d.O. Wave Energy Utilization: A Review of the Technologies. *Renew. Sustain. Energy Rev.* **2010**, *14*, 899–918. [CrossRef]
7. Prasad, K.A.; Chand, A.A.; Kumar, N.M.; Narayan, S.; Mamun, K.A. A Critical Review of Power Take-Off Wave Energy Technology Leading to the Conceptual Design of a Novel Wave-Plus-Photon Energy Harvester for Island/Coastal Communities' Energy Needs. *Sustainability* **2022**, *14*, 2354. [CrossRef]

8. Folley, M.; Curran, R.; Whittaker, T. Comparison of LIMPET Contra-Rotating Wells Turbine with Theoretical and Model Test Predictions. *Ocean Eng.* **2006**, *33*, 1056–1069. [CrossRef]
9. Falcão, A.F.O.; Sarmento, A.J.N.A.; Gato, L.M.C.; Brito-Melo, A. The Pico OWC Wave Power Plant: Its Lifetime from Conception to Closure 1986–2018. *Appl. Ocean Res.* **2020**, *98*, 102104. [CrossRef]
10. Sheng, W. Wave Energy Conversion and Hydrodynamics Modelling Technologies: A Review. *Renew. Sustain. Energy Rev.* **2019**, *109*, 482–498. [CrossRef]
11. Gallutia, D.; Tahmasbi Fard, M.; Gutierrez Soto, M.; He, J.B. Recent Advances in Wave Energy Conversion Systems: From Wave Theory to Devices and Control Strategies. *Ocean Eng.* **2022**, *252*, 111105. [CrossRef]
12. Simonetti, I.; Cappietti, L. Hydraulic Performance of Oscillating Water Column Structures as Anti-Reflection Devices to Reduce Harbour Agitation. *Coast. Eng.* **2021**, *165*, 103837. [CrossRef]
13. Cheng, Y.; Du, W.; Dai, S.; Yuan, Z.; Incecik, A. Wave Energy Conversion by an Array of Oscillating Water Columns Deployed along a Long-Flexible Floating Breakwater. *Renew. Sustain. Energy Rev.* **2024**, *192*, 114206. [CrossRef]
14. Gubesch, E.; Abdussamie, N.; Penesis, I.; Chin, C. Maximising the Hydrodynamic Performance of Offshore Oscillating Water Column Wave Energy Converters. *Appl. Energy* **2022**, *308*, 118304. [CrossRef]
15. Giorgi, G.; Gomes, R.P.F.; Henriques, J.C.C.; Gato, L.M.C.; Bracco, G.; Mattiazzo, G. Detecting Parametric Resonance in a Floating Oscillating Water Column Device for Wave Energy Conversion: Numerical Simulations and Validation with Physical Model Tests. *Appl. Energy* **2020**, *276*, 115421. [CrossRef]
16. Kim, J.S.; Nam, B.W.; Kim, S.; Park, J.; Park, S.; Kim, K.H. Experimental Study on Hydrodynamic Behavior and Energy Conversion of Multiple Oscillating-Water-Column Chamber in Regular Waves. *Ocean Eng.* **2023**, *280*, 114495. [CrossRef]
17. Liu, Z.; Xu, C.; Kim, K.; Choi, J.; Hyun, B. An Integrated Numerical Model for the Chamber-Turbine System of an Oscillating Water Column Wave Energy Converter. *Renew. Sustain. Energy Rev.* **2021**, *149*, 111350. [CrossRef]
18. Ciappi, L.; Simonetti, I.; Bianchini, A.; Cappietti, L.; Manfrida, G. Application of Integrated Wave-to-Wire Modelling for the Preliminary Design of Oscillating Water Column Systems for Installations in Moderate Wave Climates. *Renew. Energy* **2022**, *194*, 232–248. [CrossRef]
19. Henriques, J.C.C.; Portillo, J.C.C.; Sheng, W.; Gato, L.M.C.; Falcão, A.F.O. Dynamics and Control of Air Turbines in Oscillating-Water-Column Wave Energy Converters: Analyses and Case Study. *Renew. Sustain. Energy Rev.* **2019**, *112*, 571–589. [CrossRef]
20. Falcão, A.F.D.O.; Justino, P.A.P. OWC Wave Energy Devices with Air Flow Control. *Ocean Eng.* **1999**, *26*, 1275–1295. [CrossRef]
21. Falcão, A.F.O.; Henriques, J.C.C. The Spring-like Air Compressibility Effect in Oscillating-Water-Column Wave Energy Converters: Review and Analyses. *Renew. Sustain. Energy Rev.* **2019**, *112*, 483–498. [CrossRef]
22. Dimakopoulos, A.S.; Cooker, M.J.; Bruce, T. The Influence of Scale on the Air Flow and Pressure in the Modelling of Oscillating Water Column Wave Energy Converters. *Int. J. Mar. Energy* **2017**, *19*, 272–291. [CrossRef]
23. Sheng, W.; Alcorn, R.; Lewis, A. On Thermodynamics in the Primary Power Conversion of Oscillating Water Column Wave Energy Converters. *J. Renew. Sustain. Energy* **2013**, *5*, 023105. [CrossRef]
24. Şentürk, U.; Özdamar, A. Modelling the Interaction between Water Waves and the Oscillating Water Column Wave Energy Device. *Math. Comput. Appl.* **2011**, *16*, 630–640. [CrossRef]
25. Thakker, A.; Takao, M.; Setoguchi, T.; Dhanasekaran, T.S. Effects of Compressibility on the Performance of a Wave-Energy Conversion Device with an Impulse Turbine Using a Numerical Simulation Technique. *Int. J. Rotating Mach.* **2003**, *9*, 443–450. [CrossRef]
26. Gonçalves, R.A.A.C.; Teixeira, P.R.F.; Didier, E.; Torres, F.R. Numerical Analysis of the Influence of Air Compressibility Effects on an Oscillating Water Column Wave Energy Converter Chamber. *Renew. Energy* **2020**, *153*, 1183–1193. [CrossRef]
27. Elhanafi, A.; Macfarlane, G.; Fleming, A.; Leong, Z. Scaling and Air Compressibility Effects on a Three-Dimensional Offshore Stationary OWC Wave Energy Converter. *Appl. Energy* **2017**, *189*, 1–20. [CrossRef]
28. Sarmento, A.J.N.A.; De Falcao, A.F.O. Wave Generation by an Oscillating Surface-Pressure and Its Application in Wave-Energy Extraction. *J. Fluid Mech.* **1985**, *150*, 467–485. [CrossRef]
29. Weber, J. Representation of Non-Linear Aero-Thermodynamic Effects during Small Scale Physical Modeling of OWC Wave Energy Converters. In Proceedings of the 7th European Wave and Tidal Energy Conference, Porto, Portugal, 11–13 September 2007.
30. Sheng, W.; Lewis, A. Wave Energy Conversion of Oscillating Water Column Devices Including Air Compressibility. *J. Renew. Sustain. Energy* **2016**, *8*, 054501. [CrossRef]
31. Falcão, A.F.O.; Henriques, J.C.C. Model-Prototype Similarity of Oscillating-Water-Column Wave Energy Converters. *Int. J. Mar. Energy* **2014**, *6*, 18–34. [CrossRef]
32. Viviano, A.; Naty, S.; Foti, E. Scale Effects in Physical Modelling of a Generalized OWC. *Ocean Eng.* **2018**, *162*, 248–258. [CrossRef]
33. Fairhurst, J.; Van Niekerk, J.L. Modelling, Simulation and Testing of a Submerged Oscillating Water Column. *Int. J. Mar. Energy* **2016**, *16*, 181–195. [CrossRef]
34. Perez-Collazo, C.; Greaves, D.; Iglesias, G. A Novel Hybrid Wind-Wave Energy Converter for Jacket-Frame Substructures. *Energies* **2018**, *11*, 637. [CrossRef]
35. Howe, D.; Nader, J.-R.; Macfarlane, G. Experimental Analysis into the Effects of Air Compressibility in OWC Model Testing. In Proceedings of the 4th Asian Wave and Tidal Energy Conference, Taipei, Taiwan, 9–13 September 2018.
36. Benreguig, P.; Murphy, J. Modelling Air Compressibility in OWC Devices with Deformable Air Chambers. *J. Mar. Sci. Eng.* **2019**, *7*, 268. [CrossRef]

37. Rosa-Santos, P.; Taveira-Pinto, F.; Clemente, D.; Cabral, T.; Fiorentin, F.; Belga, F.; Morais, T. Experimental Study of a Hybrid Wave Energy Converter Integrated in a Harbor Breakwater. *J. Mar. Sci. Eng.* **2019**, *7*, 33. [CrossRef]
38. López, I.; Carballo, R.; Taveira-Pinto, F.; Iglesias, G. Sensitivity of OWC Performance to Air Compressibility. *Renew. Energy* **2020**, *145*, 1334–1347. [CrossRef]
39. Portillo, J.C.C.; Henriques, J.C.C.; Gato, L.M.C.; Falcão, A.F.O. Model Tests on a Floating Coaxial-Duct OWC Wave Energy Converter with Focus on the Spring-like Air Compressibility Effect. *Energy* **2023**, *263*, 125549. [CrossRef]
40. Portillo, J.C.C.; Gato, L.M.C.; Henriques, J.C.C.; Falcão, A.F.O. Implications of Spring-like Air Compressibility Effects in Floating Coaxial-Duct OWCs: Experimental and Numerical Investigation. *Renew. Energy* **2023**, *212*, 478–491. [CrossRef]
41. Ciappi, L.; Cheli, L.; Simonetti, I.; Bianchini, A.; Manfrida, G.; Cappietti, L. Wave-to-Wire Model of an Oscillating-Water-Column Wave Energy Converter and Its Application to Mediterranean Energy Hot-Spots. *Energies* **2020**, *13*, 5582. [CrossRef]
42. Kharkeshi, B.A.; Shafaghat, R.; Jahanian, O.; Alamian, R.; Rezanejad, K. Experimental Study of an Oscillating Water Column Converter to Optimize Nonlinear PTO Using Genetic Algorithm. *Energy* **2022**, *260*, 124925. [CrossRef]